JACS JOURNAL OF THE AMERICAN CHEMICAL SOCIETY

Article

Cite This: J. Am. Chem. Soc. 2018, 140, 15712−15723

pubs.acs.org/JACS

Finding and Fixing Traps in II−VI and III−V Colloidal Quantum Dots: The Importance of Z-Type Ligand Passivation

Nicholas Kirkwood,*[,†,§] Julius O. V. Monchen,[†,§] Ryan W. Crisp,[†] Gianluca Grimaldi,[†] Huub A. C. Bergstein,[†] Indy du Fossé,[†] Ward van der Stam,[†] Ivan Infante,[‡] and Arjan J. Houtepen*[,†]

[†]Optoelectronic Materials Section, Faculty of Applied Sciences, Delft University of Technology, Van der Maasweg 9, 2629 HZ Delft, The Netherlands

[‡]Department of Theoretical Chemistry, Faculty of Science, Vrije Universiteit Amsterdam, de Boelelaan 1083, 1081 HV Amsterdam, The Netherlands

Supporting Information

ABSTRACT: Energy levels in the band gap arising from surface states can dominate the optical and electronic properties of semiconductor nanocrystal quantum dots (QDs). Recent theoretical work has predicted that such trap states in II−VI and III−V QDs arise only from two-coordinated anions on the QD surface, offering the hypothesis that Lewis acid (Z-type) ligands should be able to completely passivate these anionic trap states. In this work, we provide experimental support for this hypothesis by demonstrating that Z-type ligation is the primary cause of PL QY increase when passivating undercoordinated CdTe QDs with various metal salts. Optimized treatments with $InCl_3$ or $CdCl_2$ afford a near-unity (>90%) photoluminescence quantum yield (PL QY), whereas other metal halogen or carboxylate salts provide a smaller increase in PL QY as a result of weaker binding or steric repulsion. The addition of non-Lewis acidic ligands (amines, alkylammonium chlorides) systematically gives a much smaller but non-negligible increase in the PL QY. We discuss possible reasons for this result, which points toward a more complex and dynamic QD surface. Finally we show that Z-type metal halide ligand treatments also lead to a strong increase in the PL QY of CdSe, CdS, and InP QDs and can increase the efficiency of sintered CdTe solar cells. These results show that surface anions are the dominant source of trap states in II−VI and III−V QDs and that passivation with Lewis acidic Z-type ligands is a general strategy to fix those traps. Our work also provides a method to tune the PL QY of QD samples from nearly zero up to near-unity values, without the need to grow epitaxial shells.

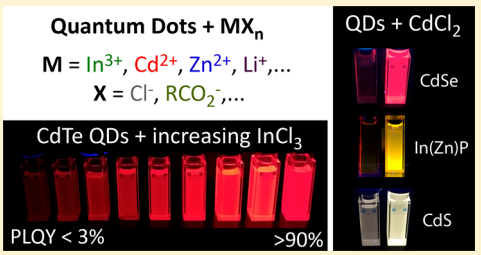

INTRODUCTION

Colloidal quantum dots (QDs) have been the focus of a substantial body of research due to their size-dependent optoelectronic properties. States in the band gap that lead to localization of charge carriers (trapping) can strongly influence optoelectronic properties in these QDs and are typically attributed to the presence of undercoordinated surface atoms. Consequently, control over these trap states remains an outstanding challenge in the field. Until recently theoretical understanding of the exact chemical nature of surface traps was limited, and as a result, efforts to add or remove trap states in QDs have been largely empirical in nature. In this work, we experimentally test the latest theoretical models of trap formation in II−VI and III−V QDs. In doing so we verify the chemical nature of the traps affecting the photoluminescence quantum yield (PL QY) and develop a general strategy to reduce their density by ligand passivation. This approach affords core-only QDs with near-complete passivation and near-unity PL QYs.

Existing experimental studies on the control of trap states have focused on the effect of adding[1−9] or removing[10−12] organic ligands on the photoluminescence (PL) of II−VI metal chalcogenide QDs, which is highly sensitive to the presence of traps. Unfortunately, these and other studies in the literature do not offer a consistent description of the relationship between trap states and the chemistry of the bond formed between ligands and surface atoms. For example, it is known that amines increase PL QYs of CdSe QDs up to 15−20% at saturation coverage[6] and that Se-rich CdSe QDs exhibit PL QYs up to 50% with addition of phosphine ligands.[7] These results are usually rationalized by considering a simplified molecular orbital analysis of a Cd−Se bond, which predicts that lone-pair electrons on Se or empty orbitals on Cd ("dangling bonds") will leave trap states in the band gap. While this predicts amines or phosphines can act as a Lewis base to fill the dangling bond on a Cd site, it is not clear why maximum PL QY values are higher for the Se-rich QDs with phosphine passivation compared to Cd-rich QDs with amine passivation.[7] Furthermore, a general understanding of the

Received: July 31, 2018
Published: October 30, 2018

DOI: 10.1021/jacs.8b07783
J. Am. Chem. Soc. 2018, 140, 15712−15723

requirements for *complete* trap passivation is not available. Reports of core-only QDs with near 100% PL QY exist, e.g., by treatment of QDs with several ligands at once[8] or via highly optimized syntheses,[13] but the precise ligands and surface sites responsible for the lack of trap states remain ambiguous, and it is not clear if there is any generality between different QD materials or crystal structures. As a result, a general experimental strategy to tune trap densities in colloidal QDs is lacking.

Density functional theory (DFT) calculations have led to an improved understanding of the origin of surface traps in QDs.[14−19] Recently, we have demonstrated that in undoped and charge-balanced nanocrystals only dicoordinated surface chalcogenide atoms should contribute to an electronic state within the band gap for zincblende II−VI nanocrystals.[20] This argument is ultimately based on orbital symmetry and can be expanded to other tetracoordinated (e.g., wurtzite) semiconductor QDs such as the III−V family and invites the prediction that the only requirement to achieve a trap-free QD should be a surface free of dicoordinated anions.

The other important factor in understanding QD passivation is an accurate, atomistic description of the bond formed between a ligand and the QD surface. Some progress has been made by adoption of the covalent bond classification (CBC) method proposed by Green[21] for metal−organic complexes.[22] This formalism categorizes ligands into three classes based on the nature of the resulting bond formed to the QD surface site. Z-type ligands bind as a neutral two-electron acceptor (a Lewis acid) to an occupied lone pair on a surface anion site (a Lewis base). L-type ligands bind as neutral two-electron donors (Lewis bases) to unoccupied surface metal orbitals (Lewis acids). Finally, X-type ligands formally share one electron with a singly occupied orbital on a surface site (covalent bond). In the QD literature, anionic ligands (e.g., Cl^-) bound to QD surfaces are often called X-type by considering a Cd^0-Cl^0 bond where each atom contributes one electron. However, this assignment is not very intuitive and highlights that complications arise when applying the CBC method to bonds with significant ionic character.

Combined with the prediction from DFT calculations that only lone pairs on dicoordinated anion sites should lead to trap states,[20] the CBC classification of ligands offers the hypothesis that Z-type ligands are the only class of ligand necessary to completely passivate trap states in QDs. Consequently only Z-type ligands should influence the PL QY, whereas X- and L-type ligands should not have any direct effect. There is already evidence for this in the literature in studies showing that the removal of Z-type ligands decreases the PL of QDs.[10−12] Most notably Saniepay et al.[11] recently concluded that the PL of CdSe QDs is much more dependent on certain Z-type binding sites than others, which supports the notion that only a fraction of surface chalcogenide sites (i.e., two-coordinated Se) are responsible for trap states. Furthermore, studies utilizing charged X-type ligands to transfer QDs from nonpolar to polar media do not result in increases of PL QY.[23−28] One study by Page et al.[8] claimed near-unity PL QYs in CdTe QDs as a result of X-type passivation of Cd sites by Cl^- anions from added $CdCl_2$, but we note that their results can be explained via Z-type passivation of Te sites by $CdCl_2$.[29,30] L-type amine ligands pose a more significant counter-argument against the hypothesis that only a two-coordinated anion results in trap states, as they are commonly observed to increase the PL QY of CdSe QDs.[6,7]

In this work we investigate the effects on PL of treatment of colloidal QDs with a wide range of Z-type ligands as well as X-type (chloride anions) and L-type (amines) ligands. We chose CdTe as a model system because it is a well-studied QD material in which we have earlier identified Te surface atoms as a source of traps,[31,32] and it has a high potential for application in solution-processable photovoltaic devices.[33−36] However, we show that our results can be generalized to other II−VI and III−V nanocrystals. We present a set of experiments demonstrating that trap states in CdTe nanocrystals can be almost completely removed by the binding of a wide range of metal halide or metal carboxylate Z-type ligands. Our results point toward the presence of a single binding energy between Z-type ligands and PL QY-active surface sites, hence suggesting that a single Te trap site is responsible for the PL QY. However, we find that ligands outside the Z-type classification such as amines and alkylammonium chlorides can also result in small but significant PL increases. This shows that the QD surface is complex and dynamic, and we discuss the implications of this result for the hypothesis that *only* dicoordinated anions can form trap states.

METHODS

Materials. All anhydrous materials and QDs were stored and handled in a nitrogen-filled glovebox atmosphere and/or using air-free Schlenk line techniques. Cadmium(II) oxide (CdO, anhydrous, 99.5%), tellurium (Te powder, 99.8%), tetradecylphosphonic acid (TDPA, 97%), palmitic acid (≥99%), trioctylphosphine (TOP, anhydrous, 97%), butylamine (99.5%), octylamine (99%) sodium caprylate (≥99%), sodium palmitate (≥98.5%), cadmium chloride ($CdCl_2$, anhydrous, 99.99%), indium chloride ($InCl_3$, anhydrous, 99.999%), zinc chloride ($ZnCl_2$, anhydrous, 99.999%), zinc bromide ($ZnBr_2$, anhydrous, 99.999%), zinc iodide (ZnI_2, anhydrous, 99.999%), magnesium chloride ($MgCl_2$, anhydrous, 99.999%), lithium chloride (LiCl, anhydrous, ≥99%), gallium(III) chloride ($GaCl_3$, anhydrous, 99.99%), aluminum chloride ($AlCl_3$, anhydrous, 99.99%), zinc acetate ($Zn(OAc)_2$, 99.99%), indium acetate ($In(OAc)_3$, anhydrous, 99.99%), cadmium acetate ($Cd(OAc)_2$, anhydrous, 99.995%), lead chloride ($PbCl_2$, anhydrous, 99.999%), gold chloride (AuCl, 99.9%), platinum chloride ($PtCl_2$, ≥99.9%), and palladium chloride ($PdCl_2$, ≥99.9%) were purchased from Sigma-Aldrich and used without further purification. Oleic acid (OA, ≥93%, Sigma-Aldrich), octadecene (ODE, 90%, Sigma-Aldrich), and oleylamine (OAM, 90%, Acros Organics) were degassed at 100 °C for 1 h before storage in a nitrogen glovebox. All solvents (toluene, methanol, hexane, acetone, and methyl acetate) were purchased anhydrous from Sigma-Aldrich and used without further purification. Rhodamine 6G and rhodamine 101 reference dyes were obtained from Lambda Physik GmbH.

Preparation of TOP-Te Precursor. A 1 M solution of TOP−Te in TOP was prepared by heating 2.553 g of Te in 20 mL of TOP to ∼150−200 °C in a N_2-filled glovebox until a clear yellow liquid was obtained. In a separate vial, 0.2 mL of this 1 M TOP−Te solution was diluted by addition of 0.8 mL of TOP and 1.0 mL of ODE, giving a final Te concentration of 0.1 M.

Synthesis of CdTe NCs. Cadmium telluride nanocrystals were synthesized according to a protocol described by Wang et al.[37] All synthesis and washing steps were carried out under an inert atmosphere and with anhydrous solvents. Briefly, CdO (25.6 mg, 0.2 mmol), tetradecylphosphonic acid (140 mg, 0.5 mmol), and ODE (4 mL) were loaded into a three-neck round-bottom flask and attached to a Schlenk line. Water and oxygen were removed by heating the flask to 100 °C under vacuum (<1 mbar) for 1 h. The solution was heated to 315 °C until a clear Cd−TDPA complex formed, then cooled to 290 °C, at which point 2 mL of a 0.1 M solution of TOP−Te in TOP and ODE was swiftly injected. After a growth time of 2−15 min depending on the desired QD size, the

DOI: 10.1021/jacs.8b07783
J. Am. Chem. Soc. 2018, 140, 15712−15723

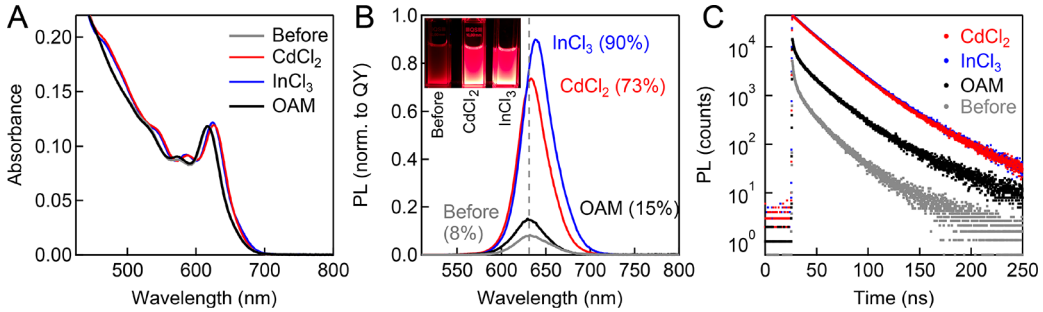

Figure 1. Optical characterization of CdTe QDs (3.8 nm diameter, 0.456 μmol/L in toluene) before and after treatment at 95 °C for 15 min with $CdCl_2$ and $InCl_3$ (630 μmol/L, equivalent to 30 ligands *added* per nm^2 CdTe surface area) with 9 equiv of OAM (5.67 mmol/L). An OAM control experiment (6.3 mmol/L, 300 ligands/nm^2) is also shown; it overlaps with the original spectrum. (A) Absorption spectra and (B) PL spectra of CdTe QDs before and after treatment with each ligand. PL QY values determined via reference dye method are shown in brackets next to the PL spectrum for each sample. Inset of (B) shows photographs of CdTe QD solutions under UV illumination before and after treatment with $CdCl_2$ and $InCl_3$. (C) Time-resolved PL traces of the same samples (60 s acquisition time).

solution was rapidly cooled and the QDs were washed twice via extraction with 10 mL of a 1:1 by volume methanol−hexane mixture at 50 °C,[38] followed by precipitation with methyl acetate and redispersion with toluene.

Preparation of MX_n−Amine Stock Solutions. Stock solutions of MX_n−amine (e.g., $CdCl_2$−oleylamine) were made by dissolving 1 mmol of MX_n in 3−9 equiv of amine (oleylamine or butylamine) at 95 °C in a N_2-filled glovebox, followed by dilution to the desired concentration with toluene. Typical MX_n−amine solutions become gels or waxy solids at room temperature, so were heated to 55−70 °C to form clear solutions immediately prior to use.

Passivation of CdTe with Ligands. All passivation experiments were conducted inside a N_2-filled glovebox. Predetermined volumes of CdTe QDs in toluene and MX_n−amine ligand solutions were added to 10 mL vials and diluted in toluene to give a final volume of 3 mL, a CdTe nanocrystal concentration of 0.456 μmol/L, and a desired ligand concentration. Ligand concentrations can be expressed as mol/L or as number of ligands added per nm^2 of total CdTe surface area (added lig/nm^2; see SI for details of the calculations of QD concentration and surface area). The vials were closed and added to a preheated aluminum heating block on a hot plate set to 95 °C. A feedback loop from a thermocouple inserted into the heating block ensured constant, reproducible temperature. After 15 min the samples were removed from the heating block and allowed to cool naturally to room temperature. In samples with higher MX_n concentrations, a white precipitate appeared during cooling due to the insolubility of the excess MX_n ligand in toluene. Once cooled, the samples were passed through a 0.2 μm PTFE syringe filter to remove these precipitates.

Optical Characterization. Optical characterization was conducted using gastight cuvettes loaded in a N_2-filled glovebox. Absorbance measurements were acquired using a PerkinElmer Lambda 1050 or Lambda 40 absorbance spectrometer. Fluorescence spectra were acquired using an Edinburgh Instruments FLS980 spectrometer. Photoluminescence quantum yields were collected using a reference dye method with rhodamine 6G and rhodamine 101, depending on the QD emission wavelength.[39] The PL QY of the reference dye was calibrated using an Edinburgh Instruments integrating sphere and found to be similar to values reported in the literature.[39,40] The PL QYs of several QD samples were also checked using the integrating sphere method and found to be in good agreement with the values obtained with the reference dye method. Photoluminescence lifetimes were collected on an Edinburgh Instruments Lifespec TCSPC setup with a 400 nm pulsed laser diode excitation (<1 ns instrument response time).

Electron Microscopy and Elemental Analysis. Transmission electron microscopy (TEM) images, electron diffractograms, and energy-dispersive X-ray (EDX) spectra were acquired using a JEOL JEM1400 transmission electron microscope operating at 120 keV with a built-in EDX detector. Prior to sample deposition onto grids for TEM and EDX measurements, QDs treated with various MX_n−amine complexes were washed twice with methyl acetate and resuspended in toluene to remove any traces of unreacted ligand. Reported EDX values are averages of 3−6 measurements taken on different areas of each sample.

RESULTS AND DISCUSSION

Treatment of CdTe QDs with MX_n Lewis Acids. CdTe QDs capped with tetradecylphosphonic acid were synthesized and washed as described by Wang et al.[37] Absorption spectra, PL spectra, and PL transients of the washed QDs are shown in Figure 1 (gray traces). X-ray and electron diffraction determined the QDs to have a zincblende crystal structure (see SI, Figure S1). After washing three times the PL QY was 8%, which indicates very incomplete surface passivation.[41]

In order to test the hypothesis that Z-type ligands can remove all trap states by passivating dicoordinated Te (Te-2c) surface sites, the washed QDs were then treated with a Lewis acidic MX_n complex (where M is a Lewis acidic metal site and X is a singly negative anion) using a modification of the protocol developed by Page et al.[8] for $CdCl_2$ passivation of CdTe. Each MX_n ligand was first dissolved at 95 °C in toluene with 9 equiv of OAM to form a clear MX_n−OAM acid−base adduct.[42−44] The OAM confers solubility in nonpolar solvents, which dissolve QDs coated in hydrophobic ligands and impede the formation of free X^- anions, which can bind to Cd sites. The MX_n−OAM complex, for brevity referred to hereafter as MX_n, was then added to the CdTe QDs in toluene to give a desired ligand concentration. In this work, we typically express the ligand concentration as ligands *added* per nm^2 of total CdTe surface area, as this facilitates comparison of results between QDs of different sizes (see supplementary methods for details of this calculation), but we stress this is not the *bound* ligand density, which is expected to be at most around 3 MX_n per nm^2.[12] The mixture of CdTe QDs and MX_n ligand was heated at 95 °C for 15 min in a nitrogen-filled glovebox and afterward allowed to cool to room temperature and filtered to remove excess ligand. We find that this procedure results in a highly reproducible increase of the PL QY of up to 90% for $InCl_3$ treatment (sample-to-sample standard deviation of 3.7% and estimated 5% systematic error).[40]

In Figure 1A the absorbance and PL of the CdTe QDs are plotted before and after the treatment with $CdCl_2$ and $InCl_3$ at an *added* ligand concentration of 30 ligands/nm^2. The solvent volumes in all experiments were set to give a QD concentration

DOI: 10.1021/jacs.8b07783
J. Am. Chem. Soc. 2018, 140, 15712−15723

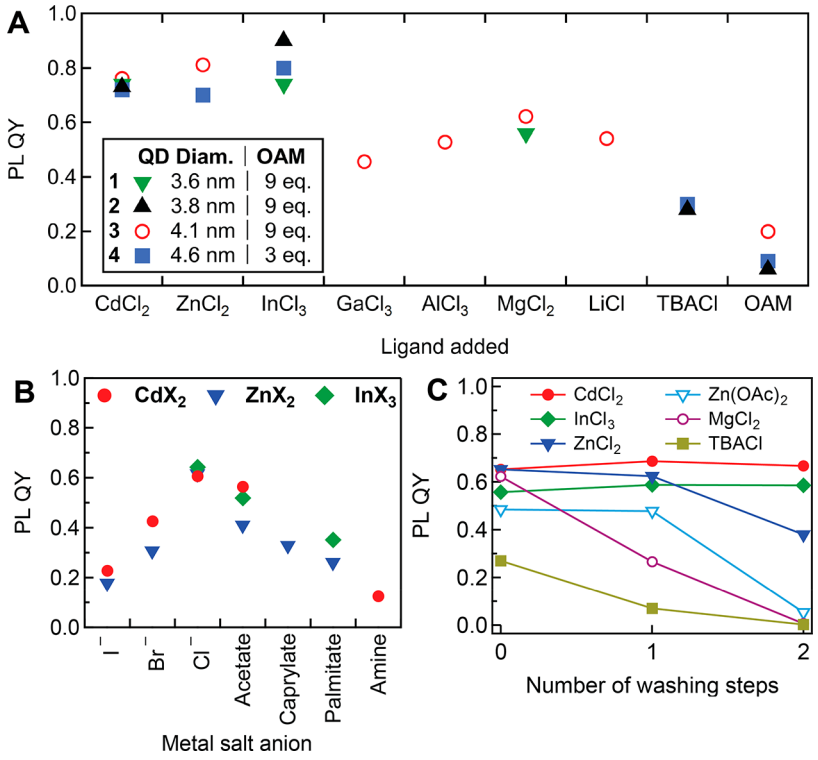

Figure 2. PL QY of CdTe QDs (0.456 μmol/L) after treatment with various MX_n-type ligands for 15 min. (A) Treatment with metal chloride ligands. Each data set utilizes different QD diameters and equivalents of OAM (per MX_n) as shown in the legend. Treatment temperature and *added* ligand concentration: 80 °C, 60 lig/nm^2 (sets 1 and 3); 95 °C, 30 lig/nm^2 (set 2); 95 °C, 14 lig/nm^2 (set 4). (B) Effect of varying anion of MX_n ligands: X = iodide (I^-), bromide (Br^-), chloride (Cl^-), acetate ($H_3C_2O_2^-$), caprylate ($H_{15}C_8O_2^-$), and palmitate ($H_{31}C_{16}O_2^-$). Treatment conditions: 4.1 nm QDs, 60 lig/nm^2 (20 lig/nm^2 for $InCl_3$), 70–85 °C, 9 equiv of OAM, 15 min. (C) PL QY of samples treated with various MX_n ligands after each of two washing steps (precipitation with methyl acetate and resuspension in toluene). Lower PL QY values in panels B and C are due to a smaller treatment volume with suboptimal temperature control (75–80 °C).

of 0.456 μmol/L. A red-shift of the absorbance and PL is observed. The treatment does not alter the width of the first absorption peak of the QDs, indicating no significant change in QD polydispersity occurred. In addition, we observe changes in the absorption spectrum for higher transitions and a small increase of absorption at the first exciton peak, all consistent with a slight increase in the effective nanocrystal diameter due to the Z-type binding of MX_n to undercoordinated Te sites on the nanocrystal surface.

Treatment of the CdTe QDs with $InCl_3$ and $CdCl_2$ resulted in a PL QY increase from 8% to 90% and 73%, respectively, clearly evident from the photo taken under UV light in the inset of Figure 1B. The PL lifetimes become significantly longer after treatment and can be fitted with a single-exponential function (lifetime 25.0 ns; see SI). This is the result of the loss of fast nonradiative decay components, indicating reduced trapping at surface defects.

In order to investigate the effects from the 9 equiv of OAM (i.e., equivalent to 270 lig/nm^2) used to solubilize the MX_n ligands, we performed a control treatment with only oleylamine at 300 added ligands/nm^2 (black traces in Figure 1A, B, and C). There was no appreciable change in the QD absorbance, but a marginal increase of the PL QY to 15% was observed and the PL lifetime became slightly longer. Although this result rules out OAM as the cause of near-unity PL QY for $CdCl_2$ and $InCl_3$, oleylamine is nonetheless able to afford a modest PL increase, despite being unable to bind to undercoordinated Te.

Optimal Treatment Conditions for Near-Unity PL QY. In general, we observed higher PL QYs after treatment with MX_n at higher temperatures (SI, Figure S2A,B), although above 100 °C more significant changes in the QD absorbance indicative of Ostwald ripening were observed. Treatment with $CdCl_2$ at 120 °C for 15 min (in ODE) gave 89% PL QY, whereas at room temperature the PL QY increased from 8% to 15% over a period of 1 h (SI, Figure S2C). This suggests that an activation barrier must be overcome for the MX_n ligand to attach to the nanocrystal surface. We tentatively attribute this to the need to dissociate the MX_n–OAM Lewis acid/base adduct to form a new Te–MX_n adduct or the rearrangement of bulky Cd–TDPA ligands from the synthesis to achieve full surface coverage. From our experiments we concluded a treatment temperature of 95 °C offers the best balance between increasing the PL QY while avoiding ripening or agglomeration of QDs, but note that each ligand has slightly different optimal conditions. True optimization was only performed for $CdCl_2$ treatment of CdTe QDs, and hence we believe treatments with other ligands and of other QDs discussed below may be optimized further.

Treatment with Other MX_n Ligands. We found that many other metal chloride treatments result in a significant increase of the PL QY of CdTe QDs under appropriate conditions (Figure 2A). We achieved the highest PL QY of 90% with $InCl_3$, and $ZnCl_2$ gave comparable results to $CdCl_2$. Other divalent ($MgCl_2$), trivalent ($GaCl_3$, $AlCl_3$), and univalent (LiCl) metal halides gave significant PL QY increases up to 60%. An increase in PL QY was also observed for

DOI: 10.1021/jacs.8b07783
J. Am. Chem. Soc. 2018, 140, 15712–15723

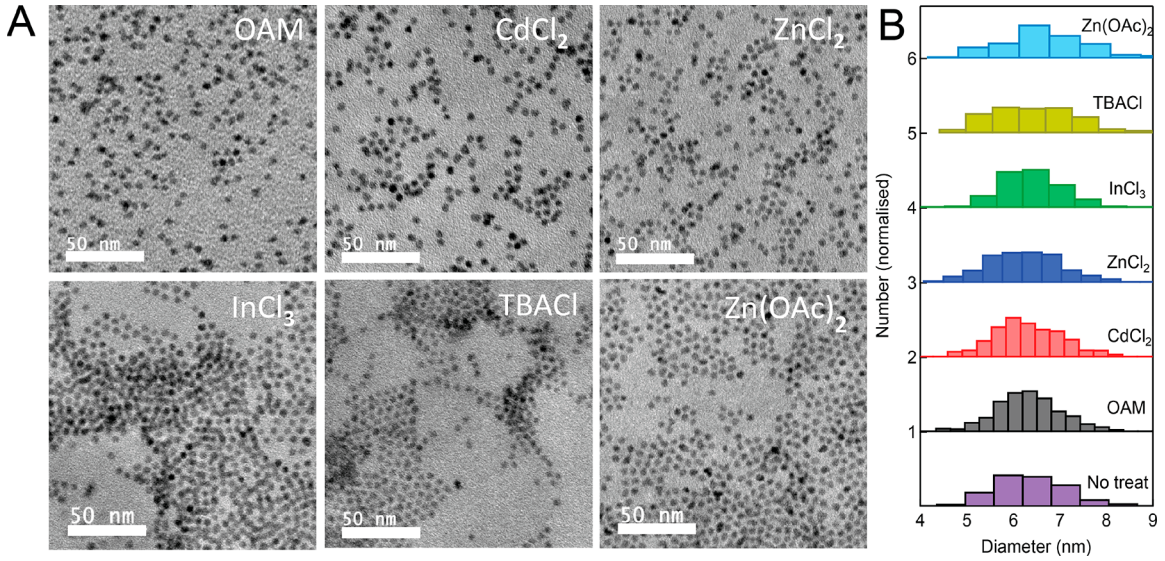

Figure 3. (A) TEM micrographs of CdTe QDs treated with various ligands. (B) Histograms of QD diameters taken from TEM micrographs.

Table 1. EDX Elemental Analysis and Cd/Te Ratios for Samples Treated with Various Ligand−OAM Complexes

	atom % (average)[a]						
element (line)	untreated	OAM	$CdCl_2$	$ZnCl_2$	$InCl_3$	$Zn(acetate)_2$	TBACl
Cd ($L_{\alpha 1}$)	56.0	55.6	59.6	32.3	33.7	46.4	50.6
Te ($L_{\alpha 1}$)	44.0	44.4	29.3	25.6	28.1	37.7	40.4
Zn ($K_{\alpha 1}$)	–	–	–	30.7	–	15.9	–
In ($L_{\alpha 1}$)	–	–	–	–	*	–	–
Cl ($K_{\alpha 1}$)	–	–	11.2	11.4	38.2	–	8.9
Total (%)	100.0	100.0	100.1	100.0	100.0	100.0	99.9
Cd/Te	1.27	1.25	2.04	1.26	1.20	1.23	1.25

[a]Values are averages from 3 to 6 measurements. *Indium content was difficult to quantify due to overlap with Te L_l and Cd $L_{\beta 1}$ signals so was omitted from quantitative analysis. "–" indicates element not detected and so not included in the analysis.

treatment with metal bromides, iodides, and carboxylates, with a general trend toward higher PL QY with shorter carboxylate carbon chains or smaller halide anions (Figure 2B). Noble metal chlorides (e.g., AgCl, AuCl, PdCl) were not compatible with this reaction system, as they were reduced by amines or the CdTe QDs themselves to give metal flakes or metal nanocrystals (SI, Figure S3C−H). Addition of lead chloride ($PbCl_2$) induced cation exchange to give PbTe QDs (SI, Figure S3B and Zhang et al.[45]).

We found that the amount of amine used to dissolve the MX_n ligand can be varied between 3 and 9 equiv with no change in the PL QY observed for MX_n treatment (Figure 2A and SI Figure S9). In addition CdTe QDs of varying diameters between 3.6 and 4.6 nm were used (Figure 2A) with very similar results, showing that the Z-type passivation is a general surface effect that can result in near-unity PL QYs independent of the QD size.

These results show clearly that the PL increase is not particular for $CdCl_2$, which was already known to enhance the PL QY of CdTe QDs and is also indispensable in the fabrication of high efficiency in CdTe solar cells, but indeed is general across all MX_n-type Lewis acids. In fact, we observe that under identical conditions the addition of $InCl_3$ increases the PL QY further than $CdCl_2$, and small metal carboxylates such as Cd, Zn, and In acetate are almost as effective as metal chlorides.

The trends in the PL QY data in Figure 2B can be explained through steric hindrance, with smaller MX_n complexes affording greater surface coverage and longer ligand chains potentially having limited accessibility to some surface sites. However, the PL QY will also be influenced by the equilibrium between bound and unbound ligand, which will be determined by the solubility of the ligand−OAM complex in the reaction solvent (toluene) and the binding affinity of the ligand. Indeed the trend toward lower PL QY with longer metal carboxylate ligands and larger, less ionic halogen salts can be understood in terms of increased solubility of the MX_n complex,[46] pushing the equilibrium toward ligand in solution. MX_n−butylamine complexes also gave rise to greater PL QY values than MX_n−OAM ones (see SI, Figure S4), consistent with the steric hindrance and solubility arguments. We explore the effect of the ligand binding affinity and equilibrium constant in more detail below.

To test the possibility that X-type binding of anions might account for these observed increases the PL QY of CdTe, we treated the CdTe QDs with tetrabutylammonium chloride (TBACl) dissolved in toluene with 9 equiv of OAM. TBACl has been reported as a source of X-type chloride ligands,[27] and the bulky alkylammonium cation lacks a Lewis acidic site to bind as a Z-type ligand to surface Te. Interestingly, TBACl treatment resulted in a reproducible PL QY increase to 30% at 14−30 lig/nm^2 irrespective of whether 3 or 9 equiv of OAM was employed (Figure 2A; for full optical characterization of

DOI: 10.1021/jacs.8b07783
J. Am. Chem. Soc. 2018, 140, 15712−15723

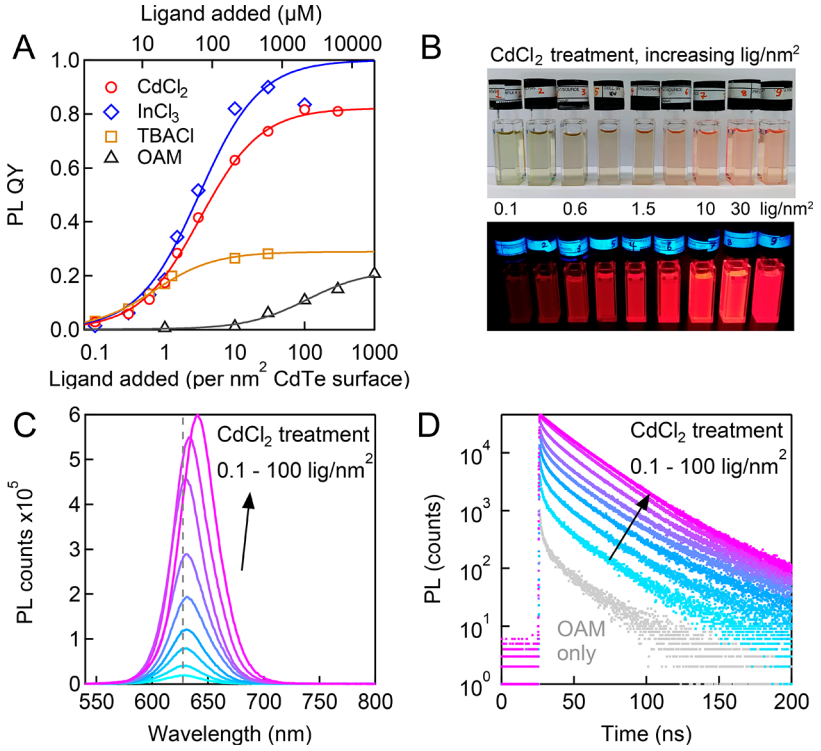

Figure 4. Effect of ligand concentration on CdTe QDs (3.8 nm, 0.456 μmol/L in toluene) after treatment at 95 °C for 15 min with $CdCl_2$, $InCl_3$, TBACl (9 equiv of OAM), and OAM only ligand. (A) PL QY of CdTe QDs after treatment with ligands as a function of concentration of added ligand per nm^2 of total CdTe surface area. Top axis shows the final ligand concentration in the solution. Lines are fits using eq 7 (see text). (B) Photographs under ambient room light (top) and UV light (bottom) showing effect of $CdCl_2$ treatment at increasing $CdCl_2$ concentrations (in nm^{-2}) on QD PL. (C) PL spectra of $CdCl_2$-treated QDs at increasing amounts of ligand added from 0.1 to 100 lig/nm^2. Dashed gray line shows position of PL peak before treatment. (D) PL decay curves of $CdCl_2$-treated QDs as a function of ligand concentration.

TBACl treatment see SI, Figure S5). This PL increase is significantly greater than that of OAM-only-treated samples even at high OAM concentrations (300 lig/nm^2). This somewhat surprising observation will be discussed further below.

QD Morphology and Composition. We investigated changes in QD morphology and composition during the treatment, as it is known that chloride salts facilitate grain growth of CdTe crystals.[35,36,47] Samples were washed two times after ligand treatment to remove excess unbound ligands and studied using TEM and EDX. We note that the PL of $CdCl_2$- and $InCl_3$-treated samples was unaltered after each washing step (see Figure 2C), suggesting that these ligands were tightly bound to the surface. $ZnCl_2$-, $Zn(acetate)_2$-, and TBACl-treated samples exhibited PL decreases during washing, suggesting loss of ligand in these samples.

The results in Figure 3 show that the QDs do not undergo any observable change in shape or diameter after treatment with a variety of ligands. EDX results in Table 1 show that all but one sample gave a Cd/Te ratio of about 1.25, which falls into a typical range for EDX measurements on II–VI QDs giving cation/anion ratios of 1.2–1.5.[7,48,49] The only exception is the $CdCl_2$-treated sample with a Cd/Te ratio of 2.04. As expected, zinc was observed in samples treated with $ZnCl_2$ and $Zn(acetate)_2$. Indium was also observed in samples treated with $InCl_3$ (Table 1), although quantification was not possible due to overlap with Te L_l and Cd $L_{\beta 1}$ spectral lines. Chlorine was measured in all samples treated with a chloride salt. We note that the Zn/Cl ratio does not match the expected 2:1, and the amount of Zn or extra Cd present in the $ZnCl_2$- or $CdCl_2$-treated samples (respectively) is much higher than would be expected for a monolayer on the QD surface. These discrepancies may reflect the lack of sensitivity toward lighter elements in EDX measurements or excess MX_n ligand loosely attached to the QDs. XPS measurements corroborate the presence of metal and chloride ions in each sample (see SI, Figure S6).

These TEM and EDX results show that the QDs are Cd-rich prior to treatment, probably due to Cd-phosphonate ligands on the surface, and the addition of MX_n ligands does not affect this ratio unless CdX_2 is used. The increase in Cd, Zn, or In content for CdX_2, ZnX_2, and InX_3 addition, respectively, confirms the addition of entire MX_n complexes onto the QD surface, rather than just the X^- anion. Comparing $Zn(acetate)_2$ and $ZnCl_2$, the higher PL QY of $ZnCl_2$-treated sample (see Figure 2B) correlates with a higher Zn content measured with EDX (Table 1), suggesting that higher PL QYs are correlated with higher Z-type ligand surface coverage.

Effect of Ligand Concentration. To further investigate the binding of each type of ligand to QD surfaces, we performed treatments with a series of increasing added ligand concentrations for $CdCl_2$, $InCl_3$, TBACl, and OAM. To avoid QD dilution each data point is taken from a separate reaction with a fixed QD concentration of 0.456 μmol/L and varying ligand concentration. In Figure 4A the PL QY is plotted as a function of *added* ligand concentration, and photographs of the samples from the $CdCl_2$ treatment under ambient and UV light are provided in Figure 4B. The PL spectra and lifetimes of the $CdCl_2$-treated samples are shown in Figure 4C,D, and for the other ligands in the SI, Figures S7 and S8.

DOI: 10.1021/jacs.8b07783
J. Am. Chem. Soc. 2018, 140, 15712–15723

Table 2. Fit Values Obtained by Fitting Eq 7 to the Data in Figure 4A

ligand	ligand type (CBC)	K (L mol^{-1})	B	Φ_{max}[a]	ΔG (kJ/mol)
$CdCl_2$	Z	$(7.78 \pm 0.37) \times 10^6$	$0.999\,67 \pm 0.000\,024$	0.83	-48.5 ± 0.2
$InCl_3$	Z	$(9.79 \pm 1.06) \times 10^6$	$1.0 \pm 0.000\,075$	1.0	-49.2 ± 0.3
TBACl	X	$(1.24 \pm 0.08) \times 10^7$	$0.9961 \pm 0.000\,13$	0.29	-50.0 ± 0.2
OAM	L	$(6.18 \pm 1.04) \times 10^4$	$0.9944 \pm 0.000\,45$	0.22	-33.8 ± 0.5

[a]Saturation PL QY predicted by the fit.

Figure 4A clearly shows that the PL QY increases with concentration for all MX_n, TBACl, and OAM ligands, but that the highest obtained PL QY (at very high ligand concentrations), as well as the functional dependence on the ligand concentration, is markedly different. The $CdCl_2$- and $InCl_3$-treated samples can be tuned from very low PL QY (under 3% at 0.1 ligand/nm^2) to near-unity values (82% at 100 lig/nm^2 for $CdCl_2$, 90% at 30 lig/nm^2 for $InCl_3$), a remarkably wide range that is clearly evident in the photographs in Figure 4B. There is also a monotonic red-shift in the PL peak position with added ligand by up to 13 nm for $CdCl_2$ (Figure 4C) and 11 nm for $InCl_3$ (see SI Figure S7), consistent with the binding of an increasing amount of Z-type ligand. Concurrent with the increase in PL QY the PL lifetimes become longer and closer to a single exponential (Figure 4D for $CdCl_2$ and SI Figure S8 for other ligands). On the other hand, TBACl treatment gives a maximum PL QY of 28% at ∼10 lig/nm^2, at which point there is only a 5 nm PL red-shift and the PL lifetime is still multiexponential (see SI, Figures S7 and S8). Oleylamine is also able to effect a PL increase up to 20% but only at very high concentrations (1000 lig/nm^2) and still exhibits multiexponential PL decay (see SI, Figures S7 and S8).

These results suggest that the binding strengths of the ligands studied in Figure 4 are different. To provide a quantitative analysis of the ligand binding strengths from the data in Figure 4A, we examine the equilibrium between added ligand and the QD surface:

$$\mathbf{S} + MX_nL_m \rightleftharpoons \mathbf{S}MX_nL_l + (m - l)L \tag{1}$$

where **S** is a QD surface site, MX_n the metal salt ligand, L the amine, and $\mathbf{S}MX_nL_l$ the bound ligand. This model assumes that all binding sites have equal affinity for ligands and takes into account the possibility that some amine (l equivalents) is not freed into solution after MX_n binds to the surface. The value of m, the number of amines coordinated to the Lewis acidic ligand in solution, has been shown to be 2 for primary amines bound to Cd-carboxylate Lewis acids.[10] The equilibrium constant K for the ligand binding can be expressed in terms of the fractional ligand surface coverage, θ:

$$K = \frac{[\mathbf{S}MX_nL_l][L]^{m-l}}{[MX_nL_m][\mathbf{S}]} = \frac{[L]^{m-l}}{[MX_nL_m]}\frac{\theta}{(1-\theta)} \tag{2}$$

If more ligand is added, $[MX_nL_m]$ increases, but due to the excess of amine utilized in these experiments (9 equiv in Figure 4A), [L] will also increase. If $m - l > 1$, then $[L]^{m-l}$ will increase more rapidly than $[MX_nL_m]$, so θ should decrease in eq 2 to maintain constant K. This situation corresponds to a net *removal* of Z-type ligands upon addition of MX_nL_m. Our data however clearly show that the PL QY (and therefore θ) increases with added ligand, meaning that $m - l < 1$. In fact, we found that the PLQY vs concentration series for $CdCl_2$ treatment in Figure 4A is identical with 3 or 9 equiv of amine (SI, Figure S9). Therefore, we conclude that the concentration of amine does not affect the binding of MX_n ligand to CdTe, i.e., $m - l = 0$. Effectively oleylamine is removed from the equilibrium, either through L-type binding to surface Cd or remaining bound to the newly added MX_n ligand. Additionally, amines can hydrogen bond to phosphonate ligands on CdTe QD surfaces,[50] and indeed ^{31}P and ^{1}H NMR experiments we conducted show that oleylamine forms adducts with native Cd-phosphonate ligands after treatment (see SI, Figure S10 and Supplementary Note 1).

Rearranging to solve for θ and setting $m - l = 0$ we get

$$\theta = \frac{K[MX_nL_m]}{K[MX_nL_m] + 1} \tag{3}$$

Previous reports have assumed that the PL QY (Φ) and surface coverage θ are linearly related,[6] but we sought to derive a relationship based on the more fundamental assumption that the number of traps is proportional to the surface coverage. Assuming all nonradiative processes arise from a single trapping process with intrinsic rate c_{trap}, the concentration of excitons N_{eh} will be governed by the rate equation

$$\frac{dN_{eh}}{dt} = -c_{trap}N_{trap}N_{eh} - k_{rad}N_{eh} \tag{4}$$

where N_{trap} is the concentration of traps and k_{rad} is the radiative recombination rate. Taking the trapping rate and concentration of traps to be time-independent quantities, $c_{trap}N_{trap}$ is a constant and eq 4 becomes a quasi-first-order rate equation. N_{eh} will therefore decay as a single exponential with the observed decay rate $k_{obs} = c_{trap}N_{trap} + k_{rad}$. We can express this rate in terms of the ligand surface coverage θ by assuming that N_{trap} is proportional to $1 - B\theta$, with B determining the maximum fraction of traps passivated at saturation (accounting for steric hindrance) and the proportionality constant given by the number of traps per QD at zero ligand coverage, N^0_{trap}:

$$k_{obs} = c_{trap}N^0_{trap}(1 - B\theta) + k_{rad} \tag{5}$$

We note that this expression offers an explanation for the deviation of a QD ensemble PL lifetime from a single exponential, in that the surface coverage and hence observed radiative rate may vary between QDs. After combining the constants c_{trap} and N^0_{trap} into a single constant c'_{trap} the PL QY will then be given by

$$\Phi = \frac{k_{rad}}{c'_{trap}(1 - B\theta) + k_{rad}} = \frac{1}{\frac{c'_{trap}}{k_{rad}}(1 - B\theta) + 1} \tag{6}$$

Finally we combine eqs 3 and 6 to obtain an expression for the PL QY in terms of the concentration of added ligand $[MX_nL_m]$:

$$\Phi = \frac{1}{\frac{c'_{trap}}{k_{rad}}\left(1 - B\left(\frac{K[MX_nL_m]}{K[MX_nL_m] + 1}\right)\right) + 1} \tag{7}$$

DOI: 10.1021/jacs.8b07783
J. Am. Chem. Soc. 2018, 140, 15712−15723

We used eq 7 to simulate the dependence of the PL QY on added ligand and found reasonable behavior for physically relevant parameters (see Supplementary Note 2 and Figure S11). We were able to measure the value of c'_{trap}/k_{rad} by measuring the PL lifetime of a CdTe QD sample with near-unity PL QY ($\theta \approx 1$; $k_{rad} \approx k_{obs}$ = 25 ns) and the average trapping lifetime of a sample with near-zero PL QY using ultrafast transient absorption spectroscopy ($\theta \approx 0$; $c'_{trap} \approx k_{obs}$ = 39.4 ps), giving a ratio of c'_{trap}/k_{rad} = 634.5 (see Supplementary Note 3 and Figure S12). Holding this ratio constant, we fit eq 7 to the data in Figure 4A (solid lines) to obtain values for fit parameters B and K (in L mol^{-1}) reported in Table 2. The free energy difference ΔG between bound and unbound ligand was also computed from the relation $\Delta G = -RT \ln K$.

$CdCl_2$ and $InCl_3$ give similar ΔG values, suggesting similar binding strengths, and TBACl is moderately higher but similar in magnitude. OAM exhibits far lower binding affinity, in line with earlier reports of weak binding of amines to II−VI QDs.[51] Our reported ΔG values suggest a very high affinity of MCl_n ligands to the QD surface, but are not unprecedented in the literature. Munro et al.[3] report ΔG values of approximately −50 kJ/mol for octadecanethiol binding to CdSe using a fitting model that relates θ to PL QY via the number of binding sites, but they note that their value of K is not unique, as they must also fit the number of binding sites. Bullen et al.[6] assumed a linear relationship between θ and PL QY and report much lower ΔG values of −24 kJ/mol (decylamine) and −26 kJ/mol (octanethiol). Clearly the model used to relate θ and PL QY has a large influence on the estimation of ΔG values. Other studies have utilized quantitative NMR to more directly measure θ when stripping Cd−carboxylate ligands from CdSe using amines and report ΔG values of cadmium carboxylate ligand binding from the amine complex in solution between +13.5 and −17 kJ/mol depending on the NC size, binding site, and the amine used.[10,11] It is instructive to compare these and our binding affinities with those reported for dissolved MX_n binding to Lewis bases in solution, which are directly measured using NMR or absorbance spectroscopy; for example, for $ZnCl_2$ in diethyl ether ΔG ranges from +4.2 kJ/mol (binding to 2-methyl-4-nitroaniline) to −20.3 kJ/mol (4-methoxybenzamide).[42] The most relevant interaction to compare these molecular ΔG values to is likely the QD−oleylamine binding affinity, for which we obtain a ΔG of −33.8 kJ/mol.

From these comparisons we tentatively conclude that our model is overestimating the binding affinity of ligands, which can be due to a number of factors. First of all, our assumed proportionality between ligand coverage and passivated trap densities (eq 5) is a continuum model that reports only an *average* ligand coverage for the ensemble; the high value of c'_{trap}/k_{rad} means that the PL QY is very sensitive to the ligand coverage around θ = 1. Thus, only a small drop in B (the maximum fraction of passivated traps) from 1 to 0.995 is required to lower the saturation PL QY value to 20% (see SI, Figure S11). We expect that a discretized binding model that accounts for the distribution of bound and unbound ligands would better model the system, especially at high ligand concentrations, and provide more accurate binding affinities. We also note that our values are sensitive to the measured c'_{trap}/k_{rad} value, so improved the understanding of these rates will also afford greater accuracy. Finally, the validity of assuming Langmuir binding, especially with a single binding energy, is potentially questionable for QDs.[52] Nonetheless, the model presented here is based on physical assumptions and measurable recombination rates and gives unique fits, which will assist with comparing results across QD samples with different nonradiative and radiative rates.

We also note that our data fits well to a single binding site model. This is particularly important in light of recent studies that have shown that there are at least two distinct ligand binding affinities for Z-type ligands to CdSe QDs arising from the heterogeneity in QD surface sites.[10,11] Saniepay et al.[11] further argued that the binding site with the highest affinity for ligands (largest $-\Delta G$ value) dominated the changes in PL when removing ligands. Because we measure the PL QY to infer the ligand binding equilibrium, we only observe the equilibrium linked to PL-sensitive surface sites. The good fits we obtain with a model assuming only one binding affinity therefore support the notion that the large majority of traps responsible for PL QY losses are associated with a single Lewis basic ligand binding site. On the other hand, the ability of non-Lewis acidic ligands (OAM, TBACl) to increase PL shows that a holistic explanation of the PL QY is not necessarily achieved through a single binding site model.

Relationship between Binding Mechanism and PL. We have demonstrated that MX_n-type Lewis acids significantly increase the PL QY of CdTe QDs up to near unity values without any observable physical change to the QDs and have shown that both the metals and anions are attached to the resulting QDs. This does not however constitute direct evidence of Z-type binding; for instance, the presence of the metal in elemental analysis can be explained as X-type binding of the anion to Cd with the metal cation providing charge compensation, i.e., a bound ion pair.[24,53] We can, however, present several counter-arguments against X-type binding being the cause of near-unity PL QY.

First, the large difference in maximum PL QY between MX_n (Lewis acid) and TBACl (no Lewis acidity) ligands supports the notion that the ability of a ligand to bind as a Lewis acid (Z-type) is most important in achieving near-unity PL QYs. Indeed, we found that samples treated with both $CdCl_2$ and TBACl gave the same PL QY as a $CdCl_2$-only-treated sample. This highlights that MX_n ligands are sufficient for achieving complete trap passivation. Second, we observed a higher PL QY for ZnX_2 ligands with a higher measured Zn content in the EDX data (Figure 2B and Table 1), so PL QY correlates with the presence of Lewis acidic metal sites. Finally, for $ZnCl_2$-treated CdTe we observed a weak signal in the nonresonant Raman spectrum at 275 cm^{-1}, which may be attributable to a Zn−Cl vibration (250 cm^{-1} in $ZnCl_2$ powder) arising from $ZnCl_2$ bound to Te (see Supplementary Note 4 and Figure S13). Therefore, we conclude that our results provide a strong argument that the majority of the PL QY increase achieved by various MX_n ligands tested is indeed due to the metal binding as a Z-type Lewis acid to undercoordinated Te sites.

However, the observations that OAM and TBACl can increase the PLQY to ∼20−30% while exhibiting markedly different affinities for the QD surface than $CdCl_2$ or $InCl_3$ need to be addressed. If we assume that TBACl can only bind to Cd as an X-type ligand and OAM as an L-type, then these results can be considered evidence against the hypothesis that *only* two-coordinated Te can contribute trap states to a QD. We propose four possibilities: (i) There are surface Cd sites that create trap states not predicted by our recent DFT calculations.[20] While we did not identify such sites, this does not disqualify their existence. One candidate is Cd−Cd dimers: it has been shown for PbS NCs that free conduction band

DOI: 10.1021/jacs.8b07783
J. Am. Chem. Soc. 2018, 140, 15712−15723

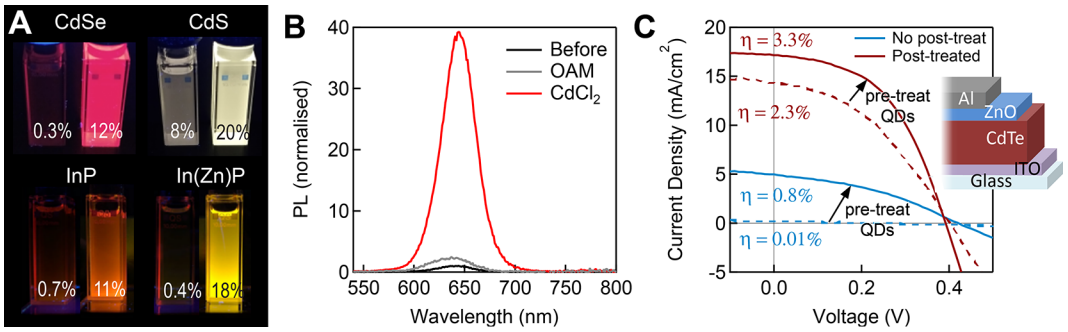

Figure 5. $CdCl_2$ treatment on other type II–VI (CdSe, CdS) and type III–V (InP, InZnP) QD materials. (A) Photographs of each QD showing before (left) and after (right) treatment with $CdCl_2$ (95 °C, 9 equiv of OAM, 15 min, 60 lig/nm^2). The PL QYs are noted for each sample. (B) PL spectra of CdSe sample from A before (black) and after (red) treatment with $CdCl_2$. Spectra are corrected for absorbance at the excitation wavelength. A control experiment with OAM only is shown in gray. (C) Current–voltage characteristics of ITO/CdTe(200 nm)/ZnO(100 nm)/Al(200 nm) solar cells. Solid lines are from devices from CdTe QDs pretreated with $CdCl_2$–octylamine complex (95 °C, 15 min, 9 equiv of amine); dashed lines from control devices from QDs heated only with octylamine. Red lines are from devices utilizing "post-treatment" of QD films by dipping into a methanolic $CdCl_2$ solution prior to sintering; blue lines from devices where QD films were directly sintered without post-treatment (see SI for further details). Arrows show effect of $CdCl_2$ pretreatment.

electrons can become trapped by populating the bonding orbital of a dynamically formed Pb–Pb dimer, which lies within the band gap.[17] A similar process might be possible for CdTe. Alternatively, for relatively large NCs facet-specific Cd surface sites, such as edge sites or adatoms, could present states in the band gap. These would not easily be found in DFT calculations on moderately sized QD model systems.[20] However, our results show that if Cd traps exist, they must contribute less to nonradiative recombination than Te traps and are removed by the addition of MX_n ligands. (ii) Some surface reconstruction follows binding of Cl or other ligands,[28] resulting in a reduction of two-coordinated Te sites. We observed no sign of morphology changes in our treatment experiments, but this does not rule out reconstruction of the QD surface. (iii) TBACl and OAM are able to passivate Te sites in a manner not well described by the covalent bond classification method. One can imagine that the tetrabutylammonium ion complexes to Te-2c surface sites. However, we have performed DFT calculations of this situation that show that the TBA cation is too bulky to influence the Te trap state enough to remove it from the band gap (see SI, Figure S14). Finally (iv) TBACl and OAM could bind to the QD and prevent diffusion of Z-type ligands across the QD surface. We have observed in molecular dynamics simulations that Z-type ligands diffuse over the QD surface. This implies that Te traps are effectively passivated only part of the time. If the density of ligands on the surface increases, the diffusion of Z-type ligands is hindered, leading to an increased time-averaged surface coverage of two-coordinated Te sites.

Which scenario, or combination of scenarios, is responsible for the increase of the PL QY with increased concentration of amines or TBACl remains unclear. What is clear is that the QD surface is a complex and dynamic system. Overall we conclude that Lewis acidic (Z-type) ligand passivation is able to remove the vast majority of surface traps responsible for the low PL QY and that our hypothesis that Te-2c surface sites are the only source of traps for CdTe QDs is mostly verified. At the same time, secondary effects are still present on the QD surface that remain not completely understood and that are not easily captured in a simple picture of passivating a single type of trap with suitable coordinating ligands.

Generalizability of Results to Other QDs and Devices. To test how general the results discussed in this work are, we performed the same treatment with $CdCl_2$ on other types of II–VI QDs and III–V QDs. Figure 5 shows the results of this treatment for CdSe, CdS, and In(Zn)P QDs. We observed a PL QY increase from 0.4% (before treatment) to 11.5% (after treatment) for CdSe QDs, whereas a control experiment with OAM only increased the PL to 0.9% (Figure 5B). A PL QY enhancement was also observed for InP and InZnP QDs[54] (Figure 5A), most notably from 0.4% to 18% for InZnP QDs. For the InZnP QDs, ligand treatment with X-type ligand (TBACl) and L-type ligand (OAM) gave no increase in the PL QY. The band-edge PL of CdS was also increased by a factor of 4 (Figure 5A), although a broad sub-band-gap PL was also enhanced (SI, Figure S15). We also observed large PL increases when treating CdTe tetrapods featuring a predominantly wurtzite crystal structure (SI, Figure S16).[33] This demonstrates that the that MX_n treatment also works for passivating undercoordinated anions on wurtzite surfaces. Achieving unity PL QY may require optimization of ligand treatment conditions for each QD material and in some cases could be hindered by the presence of defects not related to the surface.[55] However, these results suggest that Lewis acidic (Z-type) ligands are in general far more efficient than non-Lewis acidic ligands at passivating surface traps in II–VI and III–V QDs and therefore at increasing the PL QY.

Finally we stress that understanding the surface of semiconductor nanocrystals is not only of use to enhance the PL QY. Surface state passivation in general is an important scientific and technological challenge with particular relevance for semiconductor devices such as LEDs, lasers, and solar cells. To show the relation between surface state passivation on QDs and the passivation in bulk semiconductor devices, we have constructed sintered CdTe/ZnO heterojunction solar cells[35,36] from CdTe QDs that were "pretreated" with $CdCl_2$–octylamine (>100 lig/nm^2, 95 °C, 9 equiv of amine) after synthesis (Figure 5C, blue solid lines) and from control QDs treated with octylamine only (Figure 5C, blue dashed lines). The pretreatment of QDs with $CdCl_2$ increased the device efficiency from 0.01% to 0.8%. We also "post-treated" some devices with $CdCl_2$ by dipping the as-deposited CdTe QD films into a saturated solution of $CdCl_2$ in methanol before sintering;[35] while these devices showed overall higher efficiencies (red lines in Figure 5C), pretreated QDs still provided higher device efficiencies (3.3%) compared to control

DOI: 10.1021/jacs.8b07783
J. Am. Chem. Soc. 2018, 140, 15712–15723

QDs (2.3%). We observed similar results for CdTe QD devices pretreated with $InCl_3$, which will be the focus of an upcoming publication. This highlights again the generality of passivating the undercoordinated surface anions with Lewis acidic ligands. These results demonstrate that surface passivation of QDs in solution by MCl_n–amine complexes is a viable method to improve the performance of QD-based devices.

CONCLUSION

In conclusion, we have shown that CdTe QDs can be passivated with a wide range of MX_n Lewis acidic ligands, affording tunable PL QY increases up to near-unity values for optimized conditions. The PL QY of these CdTe QDs depends on the equilibrium between the MX_n ligands that are added and the surface, which is well described by a model considering only a single binding energy to the surface. These results show that the passivation of Te surface sites by Lewis acidic (Z-type) ligands is the most important factor for eliminating traps in these materials and support our recent theoretical study that two-coordinated anions are the origin of trap states in II–VI QDs. We have also found that the addition of ligands that we do not expect to bind to the two-coordinated Te trap state may increase the PL QY, albeit to significantly lower values and with a smaller binding energy. This result highlights that the QD surface is a complex and dynamic system that is not yet completely understood.

In addition we have shown that the same MX_n ligand passivation is also effective on other II–VI and III–V QDs, demonstrating that the passivation of undercoordinated anions is in general key to achieve high PL QY values in QDs. Finally, we have demonstrated that the relevance of finding and fixing traps on QD surfaces is much broader than enhancing the PL QY, by using the same ligand passivation treatment to enhance the performance of bulk CdTe solar cells made from CdTe QDs.

ASSOCIATED CONTENT

Supporting Information

The Supporting Information is available free of charge on the ACS Publications website at DOI: 10.1021/jacs.8b07783.

Supplementary methods (metal carboxylate ligand synthesis, surface area calculations, PV device fabrication); extended QD characterization (XRD, XPS, NMR, Raman spectroscopy, time-resolved spectroscopy); extended data sets for CdTe and other QD materials; calculation of radiative recombination and trapping rates from fits to TSCPC and transient absorbance data; ligand binding model simulations; and DFT calculations (PDF)

AUTHOR INFORMATION

Corresponding Authors

*A.J.Houtepen@tudelft.nl
*N.R.M.Kirkwood@tudelft.nl

ORCID

Nicholas Kirkwood: 0000-0002-7845-7081
Ryan W. Crisp: 0000-0002-3703-9617
Ward van der Stam: 0000-0001-8155-5400
Ivan Infante: 0000-0003-3467-9376
Arjan J. Houtepen: 0000-0001-8328-443X

Author Contributions

§N. Kirkwood and J. O. V. Monchen contributed equally.

Notes

The authors declare no competing financial interest.

ACKNOWLEDGMENTS

A.J.H. acknowledges support from the European Research Council Horizon 2020 ERC Grant Agreement No. 678004 (Doping on Demand). This research is supported by the Dutch Technology Foundation STW (project No. 13903, Stable and Non-Toxic Nanocrystal Solar Cells, and project No. 12734, Cadmium-free All-Inorganic Quantum Dots as Down-Conversion LED Phosphors), which is part of The Netherlands Organization for Scientific Research (NWO) (Vidi grant, No. 723.013.002), and which is partly funded by Ministry of Economic Affairs.

REFERENCES

(1) Ip, A. H.; Thon, S. M.; Hoogland, S.; Voznyy, O.; Zhitomirsky, D.; Debnath, R.; Levina, L.; Rollny, L. R.; Carey, G. H.; Fischer, A.; Kemp, K. W.; Kramer, I. J.; Ning, Z.; Labelle, A. J.; Chou, K. W.; Amassian, A.; Sargent, E. H. Hybrid passivated colloidal quantum dot solids. *Nat. Nanotechnol.* **2012**, *7* (9), 577–582.

(2) Wei, H.; Evans, C. M.; Swartz, B. D.; Neukirch, A. J.; Young, J.; Prezhdo, O. V.; Krauss, T. D. Colloidal Semiconductor Quantum Dots with Tunable Surface Composition. *Nano Lett.* **2012**, *12* (9), 4465–4471.

(3) Munro, A. M.; Plante, I.; Ng, M. S.; Ginger, D. S. Quantitative Study of the Effects of Surface Ligand Concentration on CdSe Nanocrystal Photoluminescence. *J. Phys. Chem. C* **2007**, *111* (17), 6220–6227.

(4) Kalyuzhny, G.; Murray, R. W. Ligand Effects on Optical Properties of CdSe Nanocrystals. *J. Phys. Chem. B* **2005**, *109* (15), 7012–7021.

(5) Galian, R. E.; Scaiano, J. C. Fluorescence quenching of CdSe quantum dots by tertiary amines and their surface binding effect. *Photochem. Photobiol. Sci.* **2008**, *8* (1), 70–74.

(6) Bullen, C.; Mulvaney, P. The Effects of Chemisorption on the Luminescence of CdSe Quantum Dots. *Langmuir* **2006**, *22* (7), 3007–3013.

(7) Jasieniak, J.; Mulvaney, P. From Cd-rich to Se-rich - the manipulation of CdSe nanocrystal surface stoichiometry. *J. Am. Chem. Soc.* **2007**, *129* (10), 2841–2848.

(8) Page, R. C.; Espinobarro-Velazquez, D.; Leontiadou, M. A.; Smith, C.; Lewis, E. A.; Haigh, S. J.; Li, C.; Radtke, H.; Pengpad, A.; Bondino, F.; Magnano, E.; Pis, I.; Flavell, W. R.; O'Brien, P.; Binks, D. J. Near-Unity Quantum Yields from Chloride Treated CdTe Colloidal Quantum Dots. *Small* **2015**, *11* (13), 1548–1554.

(9) Marshall, A. R.; Beard, M. C.; Johnson, J. C. Nongeminate radiative recombination of free charges in cation-exchanged PbS quantum dot films. *Chem. Phys.* **2015**, *471*, 75–80.

(10) Drijvers, E.; De Roo, J.; Martins, J. C.; Infante, I.; Hens, Z. Ligand Displacement Exposes Binding Site Heterogeneity on CdSe Nanocrystal Surfaces. *Chem. Mater.* **2018**, *30* (3), 1178–1186.

(11) Saniepay, M.; Mi, C.; Liu, Z.; Abel, E. P.; Beaulac, R. Insights into the Structural Complexity of Colloidal CdSe Nanocrystal Surfaces: Correlating the Efficiency of Nonradiative Excited-State Processes to Specific Defects. *J. Am. Chem. Soc.* **2018**, *140* (5), 1725–1736.

(12) Anderson, N. C.; Hendricks, M. P.; Choi, J. J.; Owen, J. S. Ligand exchange and the stoichiometry of metal chalcogenide nanocrystals: spectroscopic observation of facile metal-carboxylate displacement and binding. *J. Am. Chem. Soc.* **2013**, *135* (49), 18536–18548.

(13) Gao, Y.; Peng, X. Photogenerated Excitons in Plain Core CdSe Nanocrystals with Unity Radiative Decay in Single Channel: The

DOI: 10.1021/jacs.8b07783
J. Am. Chem. Soc. 2018, 140, 15712–15723

Effects of Surface and Ligands. *J. Am. Chem. Soc.* **2015**, *137* (12), 4230−4235.
(14) Califano, M. Origins of Photoluminescence Decay Kinetics in CdTe Colloidal Quantum Dots. *ACS Nano* **2015**, *9* (3), 2960−2967.
(15) Califano, M.; Gómez-Campos, F. M. Universal Trapping Mechanism in Semiconductor Nanocrystals. *Nano Lett.* **2013**, *13* (5), 2047−2052.
(16) Voznyy, O. Mobile Surface Traps in CdSe Nanocrystals with Carboxylic Acid Ligands. *J. Phys. Chem. C* **2011**, *115* (32), 15927−15932.
(17) Voznyy, O.; Thon, S. M.; Ip, A. H.; Sargent, E. H. Dynamic Trap Formation and Elimination in Colloidal Quantum Dots. *J. Phys. Chem. Lett.* **2013**, *4* (6), 987−992.
(18) Kilina, S.; Velizhanin, K. A.; Ivanov, S.; Prezhdo, O. V.; Tretiak, S. Surface Ligands Increase Photoexcitation Relaxation Rates in CdSe Quantum Dots. *ACS Nano* **2012**, *6* (7), 6515−6524.
(19) Vörös, M.; Brawand, N. P.; Galli, G. Hydrogen Treatment as a Detergent of Electronic Trap States in Lead Chalcogenide Nanoparticles. *Chem. Mater.* **2017**, *29* (6), 2485−2493.
(20) Houtepen, A. J.; Hens, Z.; Owen, J. S.; Infante, I. On the Origin of Surface Traps in Colloidal II−VI Semiconductor Nanocrystals. *Chem. Mater.* **2017**, *29* (2), 752−761.
(21) Green, M. L. H. A new approach to the formal classification of covalent compounds of the elements. *J. Organomet. Chem.* **1995**, *500* (1−2), 127−148.
(22) Owen, J. Nanocrystal structure. The coordination chemistry of nanocrystal surfaces. *Science* **2015**, *347* (6222), 615−616.
(23) Nag, A.; Kovalenko, M. V.; Lee, J.-S.; Liu, W.; Spokoyny, B.; Talapin, D. V. Metal-free Inorganic Ligands for Colloidal Nanocrystals: S2−, HS−, Se2−, HSe−, Te2−, HTe−, TeS32−, OH−, and NH2− as Surface Ligands. *J. Am. Chem. Soc.* **2011**, *133* (27), 10612−10620.
(24) Sayevich, V.; Guhrenz, C.; Dzhagan, V. M.; Sin, M.; Werheid, M.; Cai, B.; Borchardt, L.; Widmer, J.; Zahn, D. R. T.; Brunner, E.; Lesnyak, V.; Gaponik, N.; Eychmueller, A. Hybrid N-Butylamine-Based Ligands for Switching the Colloidal Solubility and Regimentation of Inorganic-Capped Nanocrystals. *ACS Nano* **2017**, *11* (2), 1559−1571.
(25) Rowland, C. E.; Liu, W.; Hannah, D. C.; Chan, M. K. Y.; Talapin, D. V.; Schaller, R. D. Thermal Stability of Colloidal InP Nanocrystals: Small Inorganic Ligands Boost High-Temperature Photoluminescence. *ACS Nano* **2014**, *8* (1), 977−985.
(26) Crisp, R. W.; Callahan, R.; Reid, O. G.; Dolzhnikov, D. S.; Talapin, D. V.; Rumbles, G.; Luther, J. M.; Kopidakis, N. Photoconductivity of CdTe Nanocrystal-Based Thin Films: Te(2-) Ligands Lead To Charge Carrier Diffusion Lengths Over 2 μm. *J. Phys. Chem. Lett.* **2015**, *6* (23), 4815−4821.
(27) Anderson, N. C.; Owen, J. S. Soluble, Chloride-Terminated CdSe Nanocrystals: Ligand Exchange Monitored by1H and31P NMR Spectroscopy. *Chem. Mater.* **2013**, *25* (1), 69−76.
(28) Marino, E.; Kodger, T. E.; Crisp, R. W.; Timmerman, D.; MacArthur, K. E.; Heggen, M.; Schall, P. Repairing Nanoparticle Surface Defects. *Angew. Chem.* **2017**, *129* (44), 13983−13987.
(29) Lewis, G. *Valence and the Structure of Atoms and Molecules*; Chemical Catalog Co.: New York, 1923.
(30) Mulliken, R. S. Molecular Compounds and their Spectra. II. *J. Am. Chem. Soc.* **1952**, *74* (3), 811−824.
(31) Boehme, S. C.; Mikel Azpiroz, J.; Aulin, Y. V.; Grozema, F. C.; Vanmaekelbergh, D.; Siebbeles, L. D. A.; Infante, I.; Houtepen, A. J. Density of Trap States and Auger-mediated Electron Trapping in CdTe Quantum-Dot Solids. *Nano Lett.* **2015**, *15* (5), 3056−3066.
(32) Boehme, S. C.; Walvis, T. A.; Infante, I.; Grozema, F. C.; Vanmaekelbergh, D.; Siebbeles, L. D. A.; Houtepen, A. J. Electrochemical Control over Photoinduced Electron Transfer and Trapping in CdSe-CdTe Quantum-Dot Solids. *ACS Nano* **2014**, *8* (7), 7067−7077.
(33) Crisp, R. W.; Panthani, M. G.; Rance, W. L.; Duenow, J. N.; Parilla, P. A.; Callahan, R.; Dabney, M. S.; Berry, J. J.; Talapin, D. V.; Luther, J. M. Nanocrystal grain growth and device architectures for high-efficiency CdTe ink-based photovoltaics. *ACS Nano* **2014**, *8* (9), 9063−9072.
(34) Panthani, M. G.; Kurley, J. M.; Crisp, R. W.; Dietz, T. C.; Ezzyat, T.; Luther, J. M.; Talapin, D. V. High efficiency solution processed sintered CdTe nanocrystal solar cells: the role of interfaces. *Nano Lett.* **2014**, *14* (2), 670−675.
(35) Jasieniak, J.; MacDonald, B. I.; Watkins, S. E.; Mulvaney, P. Solution-processed sintered nanocrystal solar cells *via* layer-by-layer assembly. *Nano Lett.* **2011**, *11* (7), 2856−2864.
(36) MacDonald, B. I.; Martucci, A.; Rubanov, S.; Watkins, S. E.; Mulvaney, P.; Jasieniak, J. J. Layer-by-layer assembly of sintered CdSe(x)Te1-x nanocrystal solar cells. *ACS Nano* **2012**, *6* (7), 5995−6004.
(37) Wang, J.; Long, Y.; Zhang, Y.; Zhong, X.; Zhu, L. Preparation of Highly Luminescent CdTe/CdS Core/Shell Quantum Dots. *ChemPhysChem* **2009**, *10* (4), 680−685.
(38) Jasieniak, J.; Smith, L.; van Embden, J.; Mulvaney, P.; Califano, M. Re-examination of the Size-Dependent Absorption Properties of CdSe Quantum Dots. *J. Phys. Chem. C* **2009**, *113* (45), 19468−19474.
(39) Würth, C.; Grabolle, M.; Pauli, J.; Spieles, M.; Resch-Genger, U. Relative and absolute determination of fluorescence quantum yields of transparent samples. *Nat. Protoc.* **2013**, *8* (8), 1535−1550.
(40) Grabolle, M.; Spieles, M.; Lesnyak, V.; Gaponik, N.; Eychmüller, A.; Resch-Genger, U. Determination of the Fluorescence Quantum Yield of Quantum Dots: Suitable Procedures and Achievable Uncertainties. *Anal. Chem.* **2009**, *81* (15), 6285−6294.
(41) Hassinen, A.; Moreels, I.; Nolf, K.; Smet, P. F.; Martins, J. C.; Hens, Z. Short-Chain Alcohols Strip X-Type Ligands and Quench the Luminescence of PbSe and CdSe Quantum Dots, Acetonitrile Does Not. *J. Am. Chem. Soc.* **2012**, *134* (51), 20705−20712.
(42) Satchell, D. P. N.; Satchell, R. S. Quantitative aspects of the Lewis acidity of covalent metal halides and their organo derivatives. *Chem. Rev.* **1969**, *69* (3), 251−278.
(43) Anderson, A.; Lo, Y. W.; Todoeschuck, J. P. Raman and Infrared Spectra of Crystals with the Cadmium Choloride Structure. *Spectrosc. Lett.* **1981**, *14* (2), 105−116.
(44) Clark, R. J. H.; Chemistry, W.-C. S. The far-infrared spectra of metal-halide complexes of pyridine and related ligands. *Inorg. Chem.* **1965**, *4* (3), 350−357.
(45) Zhang, J.; Chernomordik, B. D.; Crisp, R. W.; Kroupa, D. M.; Luther, J. M.; Miller, E. M.; Gao, J.; Beard, M. C. Preparation of Cd/Pb Chalcogenide Heterostructured Janus Particles via Controllable Cation Exchange. *ACS Nano* **2015**, *9* (7), 7151−7163.
(46) Hoerr, C. W.; Sedgwick, R. S.; Ralston, A. W. The solubilities of the normal saturated fatty acids. *J. Org. Chem.* **1946**, *11* (5), 603−609.
(47) Chambers, B. A.; MacDonald, B. I.; Ionescu, M.; Deslandes, A.; Quinton, J. S.; Jasieniak, J. J.; Andersson, G. G. Examining the role of ultra-thin atomic layer deposited metal oxide barrier layers on CdTe/ITO interface stability during the fabrication of solution processed nanocrystalline solar cells. *Sol. Energy Mater. Sol. Cells* **2014**, *125*, 164−169.
(48) Tang, J.; Kemp, K. W.; Hoogland, S.; Jeong, K. S.; Liu, H.; Levina, L.; Furukawa, M.; Wang, X.; Debnath, R.; Cha, D.; Chou, K.; Fischer, A.; Amassian, A.; Asbury, J. B.; Sargent, E. H. Colloidal-quantum-dot photovoltaics using atomic-ligand passivation. *Nat. Mater.* **2011**, *10* (10), 765−771.
(49) Brahim, N.; Mohamed, N.; Echabaane, M.; Haouari, M.; Chaâbane, R.; Negrerie, M.; Ouada, H. Thioglycerol-functionalized CdSe quantum dots detecting cadmium ions. *Sens. Actuators, B* **2015**, *220*, 1346−1353.
(50) Hassinen, A.; Gomes, R.; Nolf, K.; Zhao, Q.; Vantomme, A.; Martins, J. C.; Hens, Z. Surface chemistry of CdTe quantum dots synthesized in mixtures of phosphonic acids and amines: formation of a mixed ligand shell. *J. Phys. Chem. C* **2013**, *117* (27), 13936−13943.
(51) Fritzinger, B.; Moreels, I.; Lommens, P.; Koole, R.; Hens, Z.; Martins, J. C. In Situ Observation of Rapid Ligand Exchange in Colloidal Nanocrystal Suspensions Using Transfer NOE Nuclear

DOI: 10.1021/jacs.8b07783
J. Am. Chem. Soc. 2018, 140, 15712−15723

Magnetic Resonance Spectroscopy. *J. Am. Chem. Soc.* **2009**, *131* (8), 3024−3032.
(52) Latour, R. A. The langmuir isotherm: A commonly applied but misleading approach for the analysis of protein adsorption behavior. *J. Biomed. Mater. Res., Part A* **2015**, *103* (3), 949−958.
(53) Chen, P. E.; Anderson, N. C.; Norman, Z. M.; Owen, J. S. Tight Binding of Carboxylate, Phosphonate, and Carbamate Anions to Stoichiometric CdSe Nanocrystals. *J. Am. Chem. Soc.* **2017**, *139* (8), 3227−3236.
(54) Pietra, F.; De Trizio, L.; Hoekstra, A. W.; Renaud, N.; Prato, M.; Grozema, F. C.; Baesjou, P. J.; Koole, R.; Manna, L.; Houtepen, A. J. Tuning the Lattice Parameter of InxZnyP for Highly Luminescent Lattice-Matched Core/Shell Quantum Dots. *ACS Nano* **2016**, *10* (4), 4754−4762.
(55) Srivastava, V.; Liu, W.; Janke, E. M.; Kamysbayev, V.; Filatov, A. S.; Sun, C.-J.; Lee, B.; Rajh, T.; Schaller, R. D.; Talapin, D. V. Understanding and Curing Structural Defects in Colloidal GaAs Nanocrystals. *Nano Lett.* **2017**, *17* (3), 2094−2101.

DOI: 10.1021/jacs.8b07783
J. Am. Chem. Soc. 2018, 140, 15712−15723